Cell PRESS

Immunity
Article

Innate Immune Recognition of an AT-Rich Stem-Loop DNA Motif in the *Plasmodium falciparum* Genome

Shruti Sharma,[1] Rosane B. DeOliveira,[1,6] Parisa Kalantari,[1,6] Peggy Parroche,[1] Nadege Goutagny,[1] Zhaozhao Jiang,[1] Jennie Chan,[1] Daniella C. Bartholomeu,[2] Fanny Lauw,[1] J. Perry Hall,[3] Glen N. Barber,[4] Ricardo T. Gazzinelli,[1,2,5] Katherine A. Fitzgerald,[1,7,*] and Douglas T. Golenbock[1,7,*]

[1]Division of Infectious Diseases and Immunology, Department of Medicine, University of Massachusetts Medical School, 364 Plantation Street, Worcester, MA 01605, USA

[2]Department of Parasitology and Department of Biochemistry and Immunology, Biological Sciences Institute, Federal University of Minas Gerais, Av. Antonio Carlos 6627, Belo Horizonte, MG 31270, Brazil

[3]Department of Inflammation and Remodeling, Pfizer, Cambridge, MA 02140, USA

[4]University of Miami School of Medicine, Division of Hematology and Oncology, Department of Medicine, 1550 Northwest 10th Avenue (M710), Papanicolaou Building, Room 511, Miami, FL 33136, USA

[5]Laboratory of Immunopathology, René Rachou Institute, Oswaldo Cruz Foundation, Av. Augusto de Lima 1715, Belo Horizonte, MG 30190, Brazil

[6]These authors contributed equally to this work

[7]These authors contributed equally to this work

*Correspondence: kate.fitzgerald@umassmed.edu (K.A.F.), douglas.golenbock@umassmed.edu (D.T.G.)

DOI 10.1016/j.immuni.2011.05.016

SUMMARY

Although Toll-like receptor 9 (TLR9) has been implicated in cytokine and type I interferon (IFN) production during malaria in humans and mice, the high AT content of the *Plasmodium falciparum* genome prompted us to examine the possibility that malarial DNA triggered TLR9-independent pathways. Over 6000 ATTTTTAC ("AT-rich") motifs are present in the genome of *P. falciparum*, which we show here potently induce type I IFNs. Parasite DNA, parasitized erythrocytes and oligonucleotides containing the AT-rich motif induce type I IFNs via a pathway that did not involve the previously described sensors TLR9, DAI, RNA polymerase-III or IFI16/p204. Rather, AT-rich DNA sensing involved an unknown receptor that coupled to the STING, TBK1 and IRF3-IRF7 signaling pathway. Mice lacking IRF3, IRF7, the kinase TBK1 or the type I IFN receptor were resistant to otherwise lethal cerebral malaria. Collectively, these observations implicate AT-rich DNA sensing via STING, TBK1 and IRF3-IRF7 in *P. falciparum* malaria.

INTRODUCTION

Malaria is the world's most common infectious disease, affecting ~250 million people annually with close to 1 million deaths, mainly in children. Recurrent infections for individuals living in endemic malarial regions are common because the disease does not promote strong acquired immunity. While a combination of vector control and therapy has eliminated malaria from the wealthy countries of the world, vaccine development remains a major goal for eradication of malaria in underdeveloped countries. Much is known about the acquired immune responses to both the natural *Plasmodium* infection and a variety of immunogens (Clark et al., 2004). In contrast, little is known about the innate immune response during malaria.

The life cycle of *Plasmodium falciparum* begins in the liver. After initial replication, the parasite bursts from hepatocytes and infects erythrocytes, where cycles of asexual replication occur. The cyclic rupture of parasitized erythrocytes releases one or more malarial components ("malarial toxins") that activate phagocytes to drive inflammation resulting in systemic symptoms including fever, headaches and rigors. The molecular mechanisms involved in sensing malarial products are poorly understood.

Much progress has been made in our understanding of how phagocytes sense microbial products. The Toll-like receptor (TLR) family has been linked to the recognition of protozoan parasites (Gazzinelli et al., 2004). In humans, polymorphisms in TLR2, TLR4, TLR9, and Mal (also known as TIRAP) have been linked to the clinical outcome of malaria (Khor et al., 2007; Mockenhaupt et al., 2006). *Plasmodium* glycosylphosphatidylinositol (GPI) anchors trigger TLR2 (Zhu et al., 2005); however, GPI anchors alone cannot account for the immune stimulatory activity of malaria (Wu et al., 2010). Infected erythrocytes contain both the parasite and malaria-derived debris. During the intraerythrocytic stage, parasites digest hemoglobin and produce an inert, insoluble crystal, known as hemozoin, via a detoxification process. Natural hemozoin is coated with both proteins and plasmodial DNA and triggers TLR9 (Parroche et al., 2007; Wu et al., 2010). The ability of hemozoin to activate TLR9 is probably due to the delivery of plasmodial genomic DNA via hemozoin to the endosomal compartment. Indeed, CpG-containing DNA oligonucleotides designed from the actual sequences of malaria genome signal via TLR9 (Parroche et al., 2007). Mice deficient in *MyD88* and *Il1r-Il18r* signaling have decreased production of IL-12 and attenuated pathology during infection with murine *Plasmodium spp.* (Adachi et al., 2001; Franklin et al., 2007; Pichyangkul et al., 2004). Studies of cerebral malaria in mice

lacking TLRs have suggested that although TLRs contribute to experimental cerebral malaria (ECM), additional mechanisms also contribute (Togbe et al., 2007).

Although polymorphisms in interferon-γ (IFN-γ) receptor loci are well associated with malarial susceptibility (Koch et al., 2002; Naka et al., 2009), evidence has also linked polymorphisms in the type I IFN receptor (*Ifnar1*) (Aucan et al., 2003) to increased survival. Type I IFNs are typically generated in response to nucleic acids. Although plasmacytoid dendritic cells (pDCs) are a major source during virus infections, many cell types produce these cytokines. A number of reports have revealed the ability of *Plasmodium* to induce type I IFNs (Aucan et al., 2003; Pichyangkul et al., 2004; Vigário et al., 2007). In pDCs, TLR9 may regulate the IFN response to schizonts (Pichyangkul et al., 2004). Several additional nucleic acid sensors have also been implicated in IFN gene regulation; however, their role in malaria has not been explored to date.

In this study, we investigated the role of TLR-independent DNA sensors in type I IFN production during malaria. RNA profiling of leukocytes from febrile patients with *P. falciparum* malaria demonstrated elevated expression of interferon-inducible genes (ISGs). Although the malaria genome contains several hundred CpG motifs, and plasmodial DNA as well as schizonts have been shown to activate TLR9 (Parroche et al., 2007; Pichyangkul et al., 2004), the genome is ~80% AT (Gardner et al., 2002). In this report, we define a very common AT-rich motif in malaria, i.e., ATTTTTAC, which had previously been noted by others to be proinflammatory when isolated from probiotic bacteria (Shimosato et al., 2006). This motif is present over 6,000 times in *P. falciparum* and is also as commonly found in *P. vivax*. We used the genome of *P. falciparum* to design oligonucleotides (ODNs) that contain this AT-rich motif—these ODNs were highly immune stimulatory in both human and murine cells. AT-rich DNA activated proinflammatory cytokines such as TNF-α and IL-6 and also activated IFN-β gene transcription. We found that AT-rich DNA induced type I IFNs via a pathway that was independent of TLRs, DAI, RNA polymerase III, and IFI16/p204 but dependent on stimulator of interferon genes (STING) (Ishikawa and Barber, 2008; Zhong et al., 2008), Tank-binding kinase 1 (TBK1) (Fitzgerald et al., 2003; Ishii et al., 2008), and the interferon regulatory factors 3 (IRF3) and IRF7. Moreover, *Plasmodium*-infected RBCs also triggered IFN in macrophages via this STING-dependent pathway. Finally, mice lacking *Tbk1*, *Irf3*, and *Irf7* as well as the *Ifnar1* were resistant to lethal cerebral malaria. We suggest that this AT-rich DNA sensing pathway is important in the innate immune response to *Plasmodial* infection and determines the eventual outcome of malarial infections.

RESULTS

P. falciparum Induces Interferon Stimulated Genes during Malaria Infection

We performed global gene expression profiling of human PBMCs harvested from smear-positive symptomatic patients infected with *P. falciparum* (*Pf*), before and after curative treatment with antimalarial drugs. Patients were sick with malaria for 1–3 days (and incubating *Pf* for at least an additional week prior to symptoms) and had either a documented fever at the time of enrollment or a history of fever and/or rigors within the 24 hr period proceeding initial study. We chose to study the same patient before and after curative treatment, allowing us to measure effects due to malaria that are not compounded by other potential infections in non-malaria-infected individuals. An analysis of >580 genes induced revealed the presence of a number of ISGs, including *Aim2*, *Oas1*, *Ifitm3*, *Card12*, and *Ifitmp4* (Der et al., 1998; Sanda et al., 2006) (Figure 1A). To determine the direct effect of *Pf* on type I IFNs, we stimulated PBMCs with *Pf*-infected red blood cells (iRBCs). We found a robust induction of IFN-β mRNA. As expected, uninfected RBCs (uRBCs) did not induce IFN-β mRNA (Figure 1B). IFN-α was also induced at the protein level by iRBCs (data not shown).

We have previously demonstrated that natural hemozoin presents plasmodial DNA to TLR9 (Parroche et al., 2007). We therefore purified hemozoin and gDNA from *Pf* cultures and examined their ability to induce IFN-β. Examination of the hemozoin by microscopy confirmed that it was free of contaminating iRBC or parasites (data not shown). Cultured hemozoin induced substantial amounts of IFN-β (Figure 1C), the activity of which was lost upon DNase treatment. Like hemozoin, purified *Pf* genomic DNA (gDNA) strongly stimulated IFN-β when delivered to the cytosol of cells with cationic lipids (Figure 1C). Imaging studies showed that the hemozoin crystal was phagocytosed by macrophages and was shortly thereafter found within the lysosomal compartment (Figure 1D). At longer time points, the crystal was found localized in the cytosol, showing no lysotracker colocalization. This highlights a mechanism by which hemozoin-associated cargo such as plasmodial DNA might access the cytosol. PBMCs incubated with DNA alone in the absence of lipofectamine failed to upregulate IFN-β (data not shown). These data suggest that plasmodial genomic DNA can drive IFNβ upon access to the cytosolic compartment.

Malarial AT-Rich DNA Activates Both NF-κB- and IRF-Dependent Gene Transcription

The high AT-rich content of the malarial genome and the presence of the AT-rich motif, ATTTTTAC, found >6,000 times in *Plasmodium spp.*, prompted us to test whether this motif was immunostimulatory. The motif is found in nearly the same abundance in *P. vivax*, a species of *Plasmodium* that is not nearly so AT rich (Table S1 available online). The motif is also found in viruses, bacteria, and the human genome, albeit at lower frequencies.

We designed ODNs that contained the AT-rich motif (20-mers) with sequences derived from the malarial genome (Table S2). Like *Pf* gDNA, all six of these AT-rich motifs activated the IFN-β promoter in HEK293 cells (Figure 2A and Figure S1). ODNs designed on the basis of a portion of the genome located on *Pf* chromosome 9 containing three AT-r repeats were stimulatory in HEK293 cells or mouse macrophages (Figures 2A and 2B). Human PBMC, THP-1, mouse splenocytes, fibroblasts, bone marrow-derived macrophages (BMDM), and splenic DCs also induced IFN-β mRNA and protein in response to the AT-rich ODN (Figures 2B–2I). AT-rich DNA also induced IFN-α (data not shown) and NF-κB activation as well as cytokines like TNFα and IL-6 (Figures 2J and 2K).

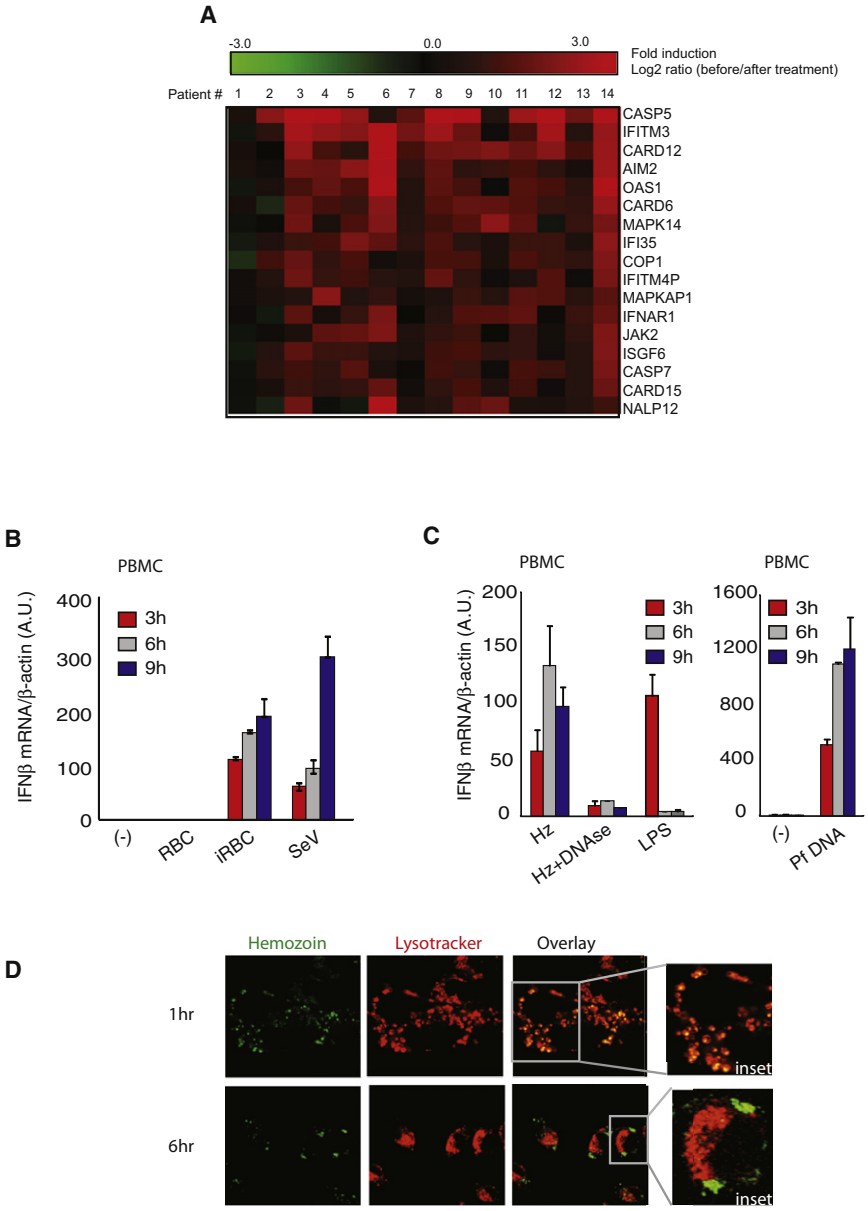

Figure 1. *P. falciparum* Induced Interferon-Stimulated Gene Expression in Human Cells

(A) A microarray analysis of PBMCs from 14 patients infected with *Pf*, before or after curative treatment with mefloquine. A selection of ISGs from a cohort of 580 upregulated genes is depicted.

(B) PBMCs were stimulated with *Pf*-infected red blood cells (iRBCs), uninfected RBCs (RBCs) or SeV (200HAU/ml) for 3 to 9 hr.

(C) PBMCs were stimulated with LPS (100ng/ml), 100 μM natural hemozoin (Hz) untreated or pretreated with *S. aureus* micrococcal nuclease (Hz + DNase) or 5 μg of genomic DNA (Pf *g*DNA) complexed with lipofectamine 2000. IFN-β and β-actin mRNA was measured by qPCR.

(D) Mouse BMDM were treated with 200 μM Hz and Hz and lysosomes were visualized with acousto-reflection microscopy and lysotracker, respectively. Fields are representative of at least ten fields of view and two independent experiments.

Secondary Structure Is a Critical Determinant of AT-Rich ODN Stimulatory Activity

We next designed a series of ODNs in which the sequences were modified (Figures S2A–S2C). Substituting the central TT with AA, so that the motif was now ATTAATAC, had little effect (Figure 3A and Figure S2A). In analyzing the active ODN using the mFold algorithm, we realized that all of the active ODNs had a stem-loop structure. Disruption of the stem-loop structure substantially reduced their activity (Figure 3B and Figure S2C). We also assessed whether single stranded-ness was a determining factor in the activity of the ODNs. When cells were stimulated with double-stranded AT-rich ODNs, we continued to see a robust activation of IFN-β. We also used the 45 bp immunostimulatory DNA (ISD) derived from the *Listeria* genome, which was annealed and prepared the same way as dsAT-rich stem loop. Only ds but not ss ISD induced a robust activation of the IFN-β reporter (Figure 3C). Structural predictions suggested that the AT-rich stem-loop DNA hybridized to the reverse strand still had secondary structure, which was not seen when ISD was analyzed in a similar manner (Figure 3C). Collectively, these data indicate that the secondary structure of the AT-rODN is the critical determinant for activity.

AT-Rich ODN Uses a Toll-like Receptor-Independent Signaling Pathway

The initial reports of AT-rich DNA elements in probiotic bacteria concluded that their activity relied on TLR9 (Shimosato et al., 2006). We have previously reported that *Pf* gDNA can signal via TLR9 (Parroche et al., 2007). To define the role of TLR9 in sensing AT-rich ODNs, we took advantage of HEK293 cell lines that either expressed or lacked TLR9. Because CpG-DNA does not trigger IFN-β in HEK293-TLR9 cells, NFκB activation was monitored in this case. *Pf* gDNA was transfected with lipofectamine 2000 or DOTAP, which target DNA to the cytosol or endosome, respectively. *Pf* gDNA (which contains both CpG and AT-rich stem-loop DNA motifs) activated NFκB when delivered to the endosomal compartment with DOTAP in TLR9-expressing HEK293 cells but not in the parental HEK293 cell line (Figure S3). In contrast, *Pf* gDNA activated NFκB in both cell lines when delivered via lipofectamine (Figure S3). These data confirm that *Pf* gDNA can engage TLR9, when delivered to the endosomal compartment, but triggers an alternative response if delivered to the cytoplasm (Figure S3).

We next tested the ability of AT-rich ODN sequences to trigger IFNβ in *Tlr9*$^{-/-}$ cells. *Pf* *g*DNA and AT-r ODN delivered via

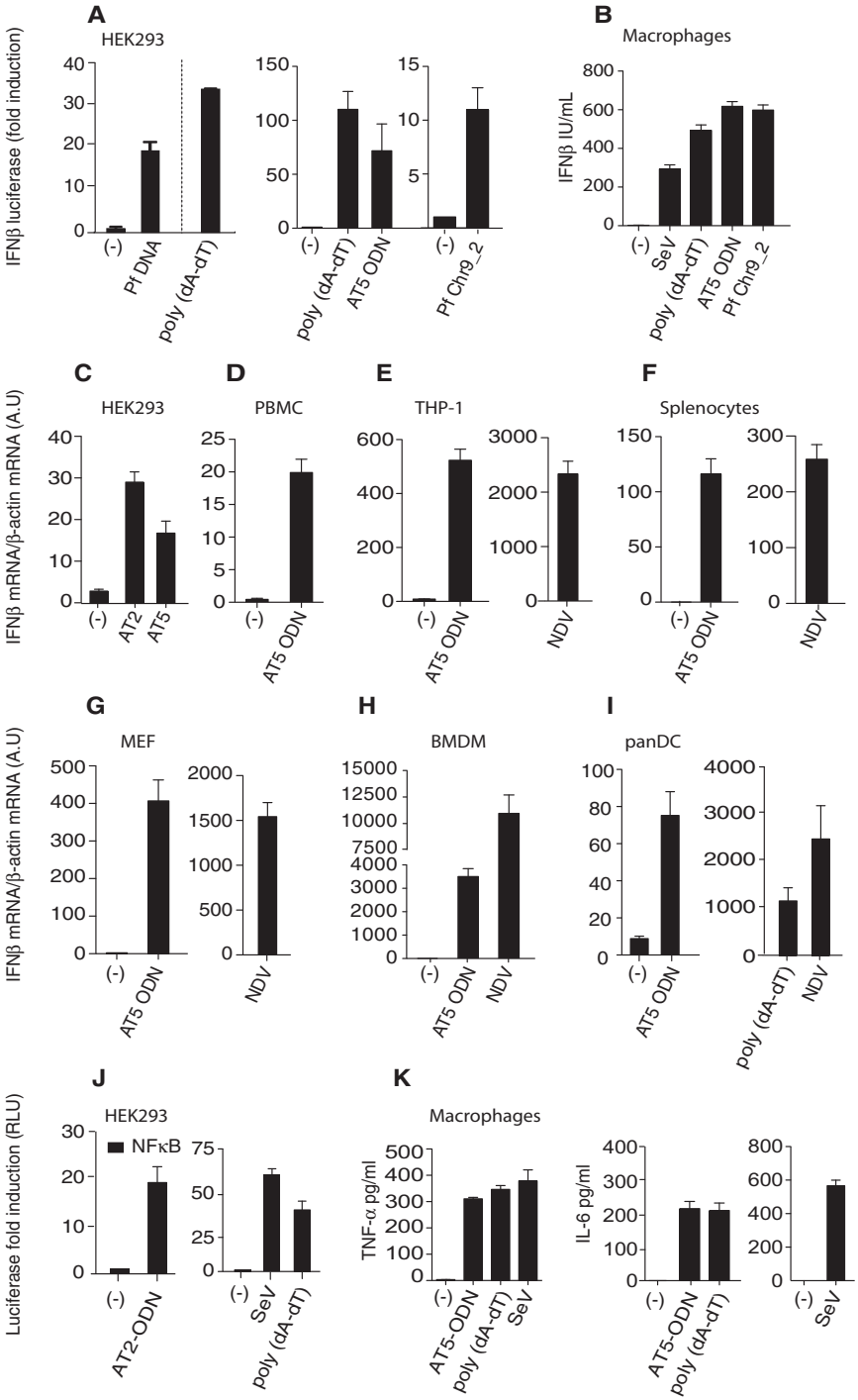

Figure 2. Immune Stimulatory Activity of AT-Rich Motifs from *P. falciparum*

(A) IFN-β reporter gene activity was measured in cells stimulated with media alone (–) or purified *Pf* g DNA (5 μg/ml), AT5 ODN (20-mer, 3 μM, phosphorothiorate backbone [PS]), *Pf* chromosomal-derived Pf Chr 9_2 long ODNs (56-mer, 3μM, PS), and poly (dA-dT) (5 μg/ml) complexed with lipofectamine 2000. Data are represented as fold induction relative to the reporter-only control and reflect mean fold induction ± SD.

(B) Bone marrow-derived macrophages (BMDMs) were stimulated with AT-rich ODNs on phosphodiester backbones (PD), SeV and pdAdT. IFN-β secretion was measured 16 hr later by ELISA.

(C–I) HEK293, PBMCs, THP-1, mouse splenocytes, embryonic fibroblasts (MEFs), BMDMs, and splenic dendritic cells (panDCs) were stimulated for 6 hr with 3 μM AT2/AT5 (PS) or AT5 (PD) and IFN-β levels measured by qPCR.

(J) NF-κB reporter gene activity in HEK293 cells stimulated with AT2 (3 μM, PS), poly (dA-dT) (5 μg/ml), or infected with SeV (200HAU/ml).

(K) IL-6 or TNFα levels were measured by ELISA from macrophages treated as indicated for 18 hr. Data are presented as mean ± SD and are representative of three independent experiments.

lipofectamine induced normal levels of IFNβ mRNA in spleens from *Tlr9*$^{-/-}$ mice (Figure 4A). Although CpG-containing ODNs induced modest amounts of type I IFN, this activity was lost in macrophages and splenocytes harvested from *Tlr9*$^{-/-}$ mice (Figure 4A and data not shown). *Myd88*$^{-/-}$*Ticam1*$^{-/-}$ splenocytes and macrophages also responded normally to the presence of cytosolically administered AT-rich ODNs and *Pf g*DNA ruling out a role for any other TLRs (Figure 4B and data not shown).

AT-Rich Stem-Loop DNA Does Not Result in the Activation of Any Known Nucleic Acid Sensor

A growing number of nucleotide receptors have been identified which includes retinoic inducible gene-I (RIG-I, encoded by *Ddx58*), melanoma differentiation associated gene-5 (Mda-5, encoded by *Ifih1*) (Kawai et al., 2005; Yoneyama and Fujita, 2009), NOD2 (Sabbah et al., 2009), and DNA-dependent activator of IFN-regulatory factors (DAI, encoded by *Zbp1*) (Takaoka et al., 2007). To examine the role of these sensors, we tested bone marrow cells that were deficient in each of these receptors. *Ifih1*$^{-/-}$, *Ddx58*$^{-/-}$, and *Mavs*$^{-/-}$ responded normally to AT-rich stem-loop DNA (Figures 4C–4E). Similar results were observed with *Nod2*$^{-/-}$ and *Zbp1*$^{-/-}$ cells (Figures 4F and 4G). The reduction of DAI expression in HEK293 cells by RNA interference also had no effect on AT-rich ODN activity (Figure 4H).

AT-Rich Stem-Loop DNA Uses a Distinct Pathway from B-Form Double Stranded Poly(dA-dT) to Induce Type I IFNs

In human cells, poly(dA-dT) drives type I IFNs via RNA polymerase III, which converts poly(dA-dT) into a ligand for the RIG-I-MAVS pathway (Ablasser et al., 2009; Chiu et al., 2009).

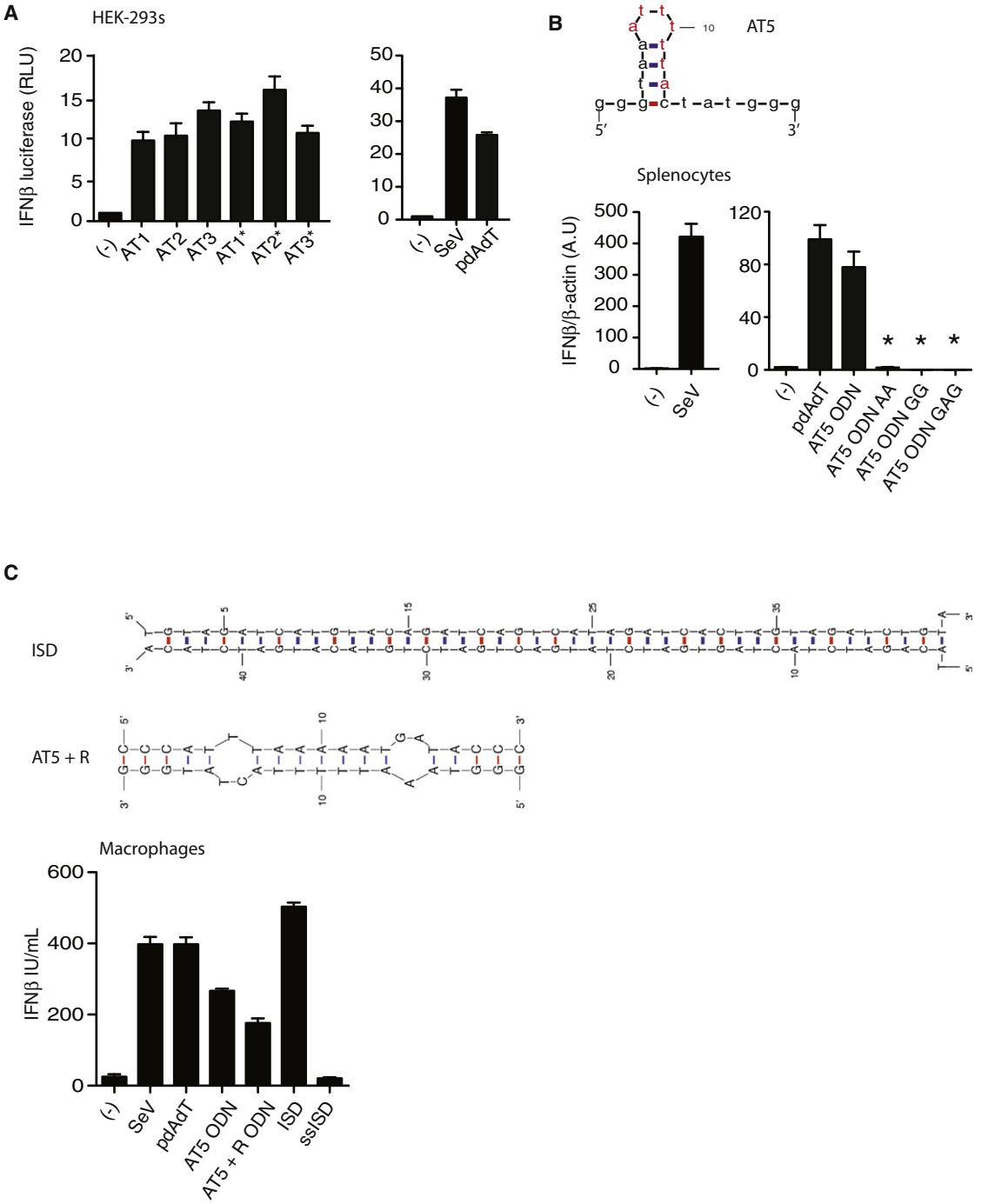

Figure 3. AT-Rich Motifs Induce IFN-β Production in a Sequence and Secondary Structure-Dependent Manner

(A) HEK293 cells transfected with the IFN-β reporter plasmid were stimulated with SeV, poly(dA-dT), and AT-rich ODNs that were modified (*) as in Figure S2A and luciferase activity was read an additional 24 hr later.

(B) Putative secondary structure of AT-rich ODN AT5, with AT-motif and probable chief base-base interactions highlighted. Key base-base interaction and secondary structure was abolished by base-directed substitution of the original sequences as shown in Figure S2B. Splenocytes from C57BL/6 mice were stimulated with the parent AT5 (3 μM, PD) and denoted base-substituted oligonucleotides and IFN-β mRNA induction measured by qPCR. NDV, NewCastle Disease Virus.

(C) Predicted secondary structure of annealed AT5 and reverse strand and ISD (3 μM each, PD). BMDMs from C57BL/6 mice were stimulated with the single stranded (ss) AT5, AT5 annealed to its reverse strand (AT5 + R), annealed ISD, and ssISD (forward strand only) for 18 hr and IFN-β secretion was measured by ELISA. Data are presented as mean ± SD and are representative of three independent experiments.

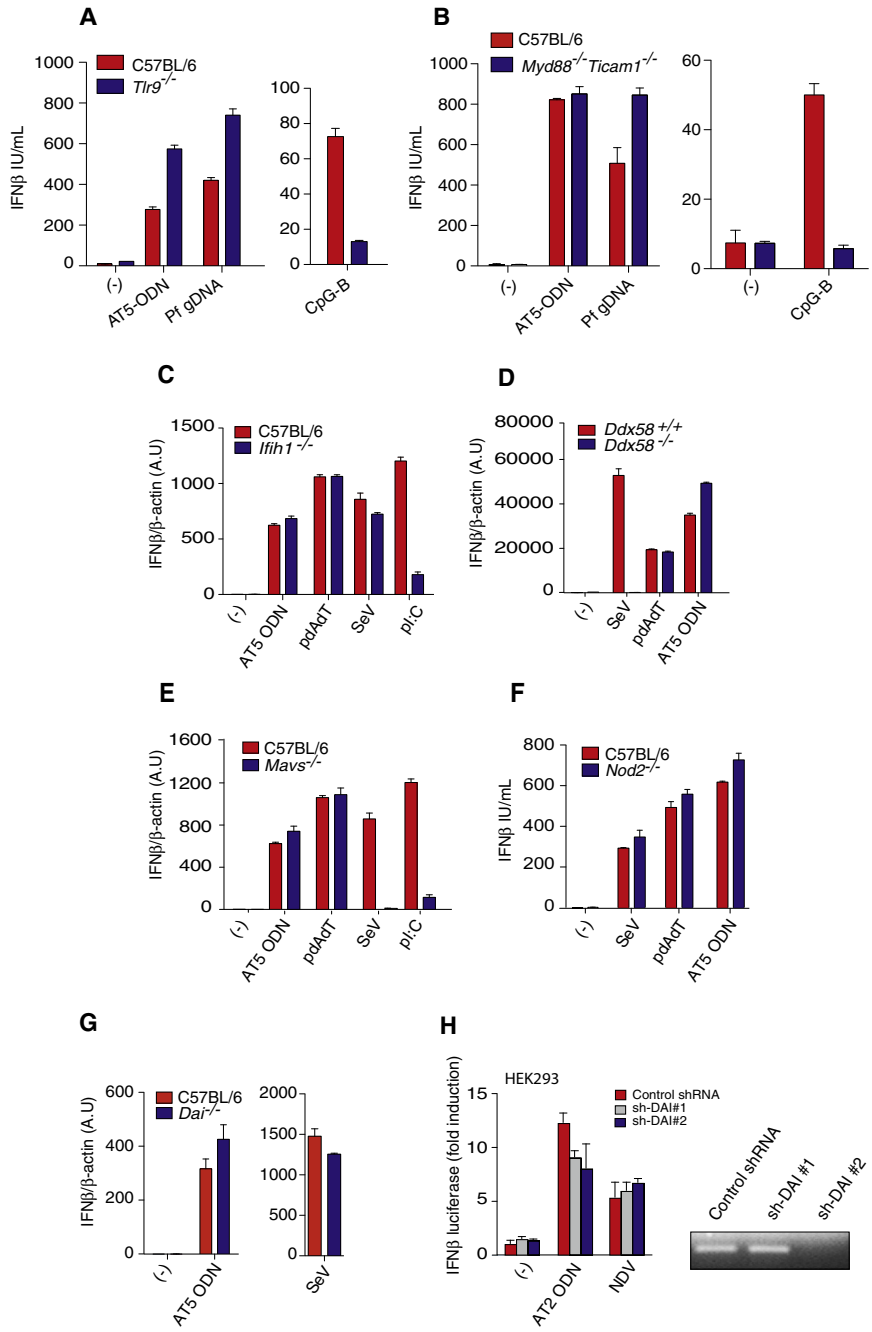

Figure 4. AT-Rich DNA Mediated IFN-β Induction Does Not Require TLRs, Cytosolic Sensors, or the Adaptor Protein MAVS

(A and B) Splenocytes from the indicated strains were stimulated with CpG-B 1826 (5 μM), AT5 (3 μM, PD), or Pf gDNA (100 ng/ml) complexed with lipofectamine 2000 for 6 hr, and IFN-β was measured by qPCR and/or ELISA.

(C–G) BMDMs from the indicated strains were stimulated with lipofectamine complexed AT5 (3 μM, PD), poly (dA-dT) (5 μg/ml), and poly (I:C) (100ng/ml) or infected with SeV (200 HAU/ml), and IFN-β mRNA measured by qPCR or ELISA.

(H) HEK293 cells were transduced with two lentiviruses encoding shRNA for DAI, and IFN-β reporter gene activity was measured from cells stimulated with lipofectamine complexed-AT2 (3 μM, PS) or infected with NDV (80HAU/ml) for 24 hr. The efficiency of DAI silencing was examined by RT-PCR. Data are presented as mean ± SD and are representative of three independent experiments.

This pathway is redundant with additional sensors in mouse macrophages. To test this pathway, we silenced RIG-I, MAVS, and RNA polymerase III component 1 (RPC1) by RNAi in HEK293 cells and measured IFN-β reporter gene activity. siRNA-mediated silencing of these components had no effect on the ability of AT-rich stem-loop DNA to induce IFN-β gene transcription (Figure 5A and Figure S4A). siRNA-mediated silencing of these components had no effect on the ability of AT-rich stem-loop DNA to induce IFN-β gene transcription. We also tested whether transfected AT-rich ODNs would result in the RNA pol III-dependent production of stimulatory RNA. RNA extracted from transfected 293 cells was tested for its ability to activate RIG-I in PBMCs. Although IFN-α was induced with small and total RNA from the poly(dA-dT) transfected cells, *Plasmodial* AT-rich stem-loop DNA did not yield a stimulatory RNA species (Figure 5B). Similarly, HEK293 cells were able to induce the activation of the IFN-β reporter in response to RNA extracted from poly(dA-dT) transfected but not in response to AT-rich stem-loop DNA-derived RNA (Figure S4B).

We also tested ML-60218, an inhibitor of RNA pol III (Ablasser et al., 2009; Chiu et al., 2009), and NS3/4A (a protease component of the Hepatitis C virus that blocks RIG-I signaling (Foy et al., 2005; Meylan et al., 2005), neither of which had any effect on AT-rich ODN-induced activation (Figures 5C and 5D). Finally, *Zbp1*-deficient macrophages treated with the RNA pol III inhibitor ML60218 (Figure 5E) responded normally to AT-rich ODNs, excluding the possibility that DAI and RNA pol III function redundantly. We confirmed these findings in HEK293 cells transfected with DAI-specific shRNA pretreated with ML60218 (Figure 5F). Recently, IFI16 was identified as a sensor of viral DNA that couples to the STING pathway (Unterholzner et al., 2010). siRNA-mediated transient knockdown of Ifi204/p204 (the murine ortholog of IFI16) prevented HSV and VACV DNA driven IFN-β induction (Figure 5G) but had no effect on AT-r stem-loop DNA (Figure 5G). Collectively, these data suggest that AT-r DNA induce IFN-β independently of all currently described DNA sensing receptors.

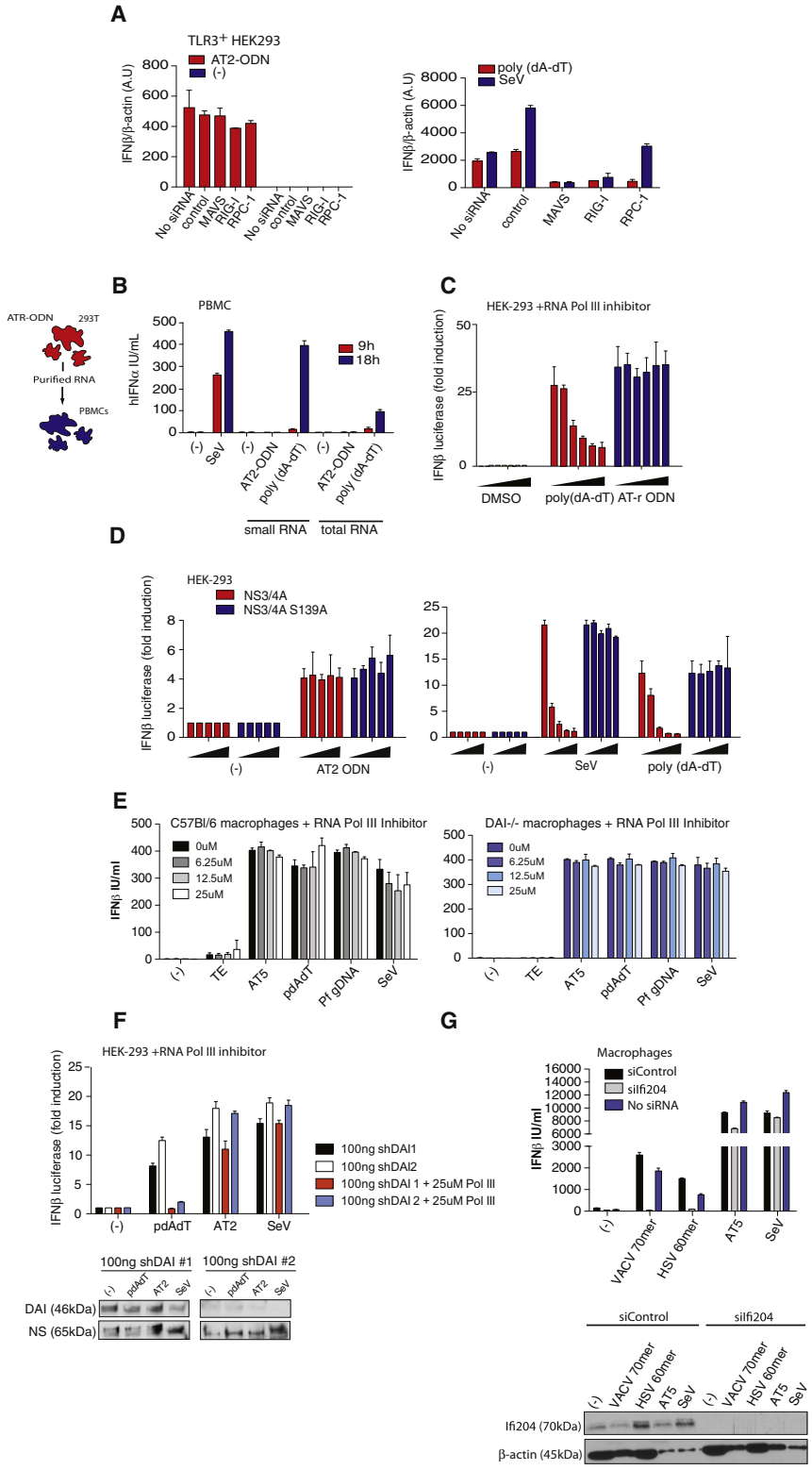

Figure 5. *P. falciparum* AT-Rich Motifs Do Not Signal via RNA-Polymerase III/RIG-I

(A) RIG-I, MAVS, and RNA polymerase III component 1 (RPC1) were silenced by RNAi. Forty-eight hours later, cells were stimulated with AT2 (PS; left side of graphic), poly (dA-dT), and SeV (right side of graphic). IFN-β gene induction was assessed 24 hr later with qPCR.

(B) HEK293 cells were transfected with either poly (dA-dT) or AT2 and RNA from the transfected cells was harvested 16 hr later. Harvested RNA was fractionated as indicated and transfected back into PBMCs and IFN-α production assessed 9 or 18 hr later.

(C) HEK293 cells were pretreated with 0, 2.5, 5, 10, 20, or 30 ng of the RNA polymerase III inhibitor, ML-60218, or vehicle alone (DMSO) for 2 hr and IFN-β reporter activity was measured after AT2 (PS) or poly (dA-dT) treatment.

(D) A total of 0, 20, 40, 60, and 80 ng of plasmids encoding the hepatitis C virus (HCV) protease NS3/4A and the inactive mutant NS3/4A S139A were transfected into HEK293 cells along with the IFN-β reporter. Twenty-four hours later, the cells were stimulated with AT2 (PS), poly (dA-dT) and SeV. Luciferase activity was assessed an additional 24 hr later.

(E) C57Bl6 or *Zbp1*$^{-/-}$ macrophages were pretreated with ML-60218 for 2 hr and then stimulated as indicated, and IFN-β levels were measured by ELISA.

(F) DAI was silenced by RNAi and cells pretreated with the ML60218 inhibitor. IFN-β reporter gene activity measured after cells were stimulated with AT2, poly(dA-dT), and Sendai virus (SEV). shRNA-mediated knockdown of DAI (*Zbp1*) was assessed with immunoblotting at 48 hr after transfection of shRNAs.

(G) Mouse macrophages were electroporated with siRNA to Ifi204 or scrambled siRNA control for 48 hr and then stimulated with indicated ligands for an additional 24 hr. Supernatants were assessed for levels of IFN-β (top) by ELISA, whereas lysates of cells were assessed for levels of Ifi204 remaining (bottom) by immunoblotting. Data are presented as mean ± SD and are representative of three independent experiments.

IFN Induction by AT-Rich Stem-Loop DNA Requires STING, TBK1, and IRF3/7

Most cytosolic DNA-induced IFN signaling pathways converge on STING (encoded by *Tmem173*) (Ishikawa and Barber, 2008; Ishikawa et al., 2009; Saitoh et al., 2009) and TBK1 (Fitzgerald et al., 2003; Ishii et al., 2008). *Tmem173*$^{-/-}$ cells were unable to induce IFN-β in response to AT-rich stem-loop DNA or *Pf* gDNA stimulation (Figure 6A). These findings were corroborated with IFN-β reporter assays in HEK293 cells transfected with STING siRNA (Figure 6B). STING deficiency also impairs the induction of a number of additional ISGs as well as NF-κB dependent cytokines such as TNF-α, IL-6, and IL-15 upon treatment with either AT-rich ODNs or *Pf* genomic DNA (Figure 6C and Figure S6). Although *Tbk1*$^{-/-}$ mice die during embryogenesis, this lethality is rescued by crossing these

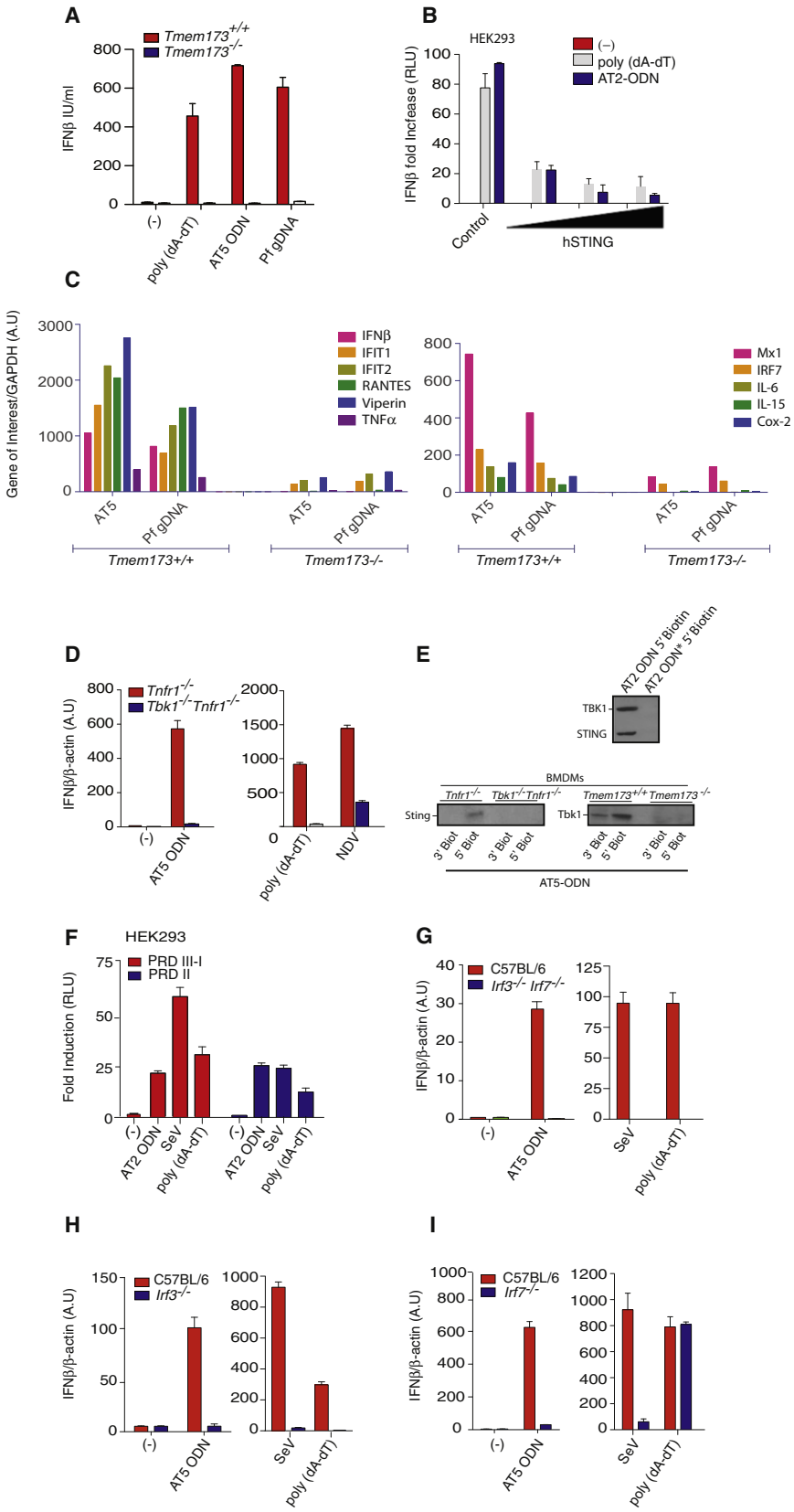

Figure 6. AT-Rich DNA-Mediated IFN-β Induction Uses the Adaptor STING, TBK1, and the Interferon Regulatory Factors IRF3 and IRF7

(A) BMDM from *Tmem173*$^{-/-}$ mice were transfected with lipofectamine complexed AT5 (3 μM, PD), Pf gDNA (100ng/ml) and poly (dA-dT) (3.5 μg/ml) or infected with SeV (200HAU/ml), and IFN-β gene induction was measured 6 hr later by qPCR.

(B) STING was silenced by siRNA and IFN-β reporter gene activity was measured after treatment with poly (dA-dT) and AT2.

(C) BMDMs from *Tmem173*$^{+/+}$ and *Tmem173*$^{-/-}$ mice were stimulated as indicated for 6 hr and gene expression was analyzed with Nano-string technology. Key genes affected are shown.

(D) *Tbk1*$^{-/-}$*Tnfr1*$^{-/-}$ and *Tnfr1*$^{-/-}$ BMDMs were treated as indicated and IFN-β mRNA levels were measured by qPCR.

(E) HEK293 cells (upper panels) or BMDMs from *Tnfr1*$^{-/-}$, *Tbk1*$^{-/-}$*Tnfr1*$^{-/-}$, *Tmem173*$^{+/+}$ and *Tmem173*$^{-/-}$ mice were transfected as indicated with biotinylated ODNs. Cell lysates were subjected to pull-down analysis, and immunoblots were probed for the presence of STING and TBK1 by immunoblotting.

(F) HEK293 cells were transfected with multimerized PRDIII-I and PRDII reporter elements from the IFN-β promoter and stimulated as above. Luciferase reporter activity was measured.

(G–I) BMDMs from *Irf3*$^{-/-}$*Irf7*$^{-/-}$, *Irf3*$^{-/-}$, and *Irf7*$^{-/-}$ mice were transfected as indicated and levels of IFN-β mRNA were quantified 6 hr later by qPCR.

mice to the *Tnfr1*$^{-/-}$ mice (Bonnard et al., 2000). We therefore also compared *Tnfr1*$^{-/-}$ and *Tbk1*$^{-/-}$*Tnfr1*$^{-/-}$splenocytes and BMDMs for AT-rich ODN-induced IFN-β gene transcription and secretion. *Tbk1*$^{-/-}$*Tnfr1*$^{-/-}$ splenocytes had a markedly reduced IFN-β response upon challenge with AT-rich ODNs (Figure 6D).

We also tagged AT-2 or AT-5 ODNs with biotin and performed streptavidin pull-down assays in lysates from HEK293 cells to examine STING-TBK1 complex formation. The labeled ODNs precipitated the STING-TBK1 complex, whereas a control non-stimulatory ODN, in which the DNA sequences were scrambled, failed to immunoprecipitate this complex (Figure 6E). The immunoprecipitation of STING appears to be dependent on TBK1 given that AT-rich ODNs precipitated STING in macrophage lysates from *Tnfr1*$^{-/-}$ mice but failed to pull down STING from lysates of *Tbk1*$^{-/-}$*Tnfr1*$^{-/-}$ mice. Moreover, TBK1 was brought down in a complex with the AT-rich ODNs in *Tmem173*$^{+/+}$ macrophages but failed to do so in *Tmem173*$^{-/-}$ macrophages. Thus, STING and TBK1 cooperatively associate in this AT-rich stem-loop DNA sensing pathway. There is a partial role for the TBK-1-related kinase IKKε in AT-rich stem-loop DNA-dependent IFN-β production (Figure S5A).

The transcriptional enhancer of the IFNβ gene contains binding sites for NF-κB: the IRFs (IRF3 and IRF7) and the heterodimeric complex ATF-2/c-Jun (Panne et al., 2007). AT-rich ODNs induced reporter gene expression from both the full-length promoter and from reporter genes driven by multimerized individual promoter elements (Figure 6F and data not shown). Activation of IRF3-IRF7 has been considered a defining event in the transcriptional regulation of the IFN-β gene (Honda and Taniguchi, 2006). IFN-β induction was severely abrogated in splenocytes from *Irf3*$^{-/-}$*Irf7*$^{-/-}$ double knockout (DKO) mice well as from the single KOs after treatment with AT-rich ODNs (Figures 6G–6I). This result suggests that AT-rich stem-loop DNA from *Plasmodium* most likely activates type I IFN induction via IRF3 and IRF7 heterodimers. IRF1 and IRF5 were dispensable for AT-rich ODN-mediated IFN-β induction (Figures S5B and S5C).

To examine the physiological relevance of this pathway to malaria infection, we conducted a series of ex vivo experiments in which parasitized RBCs (*P. berghei ANKA*-infected RBCs [*PbA* iRBCs] or *Pf* iRBCs) were incubated with mouse macrophages from either wild-type mice or mice deficient in key components of the cytosolic AT-rich pathway identified above. Macrophages from *Irf3*$^{-/-}$*Irf7*$^{-/-}$ or *Tbk1*$^{-/-}$*Tnfr1*$^{-/-}$ mice failed to induce IFN-β in response to purified *Pf* iRBCs. A similar defect was seen when *PbA* iRBCs were introduced to *Tbk1*$^{-/-}$*Tnfr1*$^{-/-}$ *or Irf3*$^{-/-}$*Irf7*$^{-/-}$ cells (Figures 7B and 7C). We also compared wild-type and *Tmem173*$^{-/-}$ cells and as seen in Figure 7D, STING-deficiency led to a partial but significant defect in type I IFN responses in response to *PbA* iRBCs.

TBK1-IRF Dependent Type I Interferon Pathway Is Central to the Pathogenesis of Experimental Cerebral Malaria

We next wanted to test whether this pathway was important in plasmodial infection in vivo. *P. berghei* ANKA (*PbA*) causes cerebral malarial disease in mice. The model reflects many of the signs of human cerebral malaria, including lethargy, limb paresis-paralysis, vestibular dysfunction, coma, and death, and is a useful model for assessing the contribution of host factors in the pathogenesis of severe malaria (Neill and Hunt, 1992). Susceptible strains of mice, when infected with blood stage forms of *P. berghei* ANKA, rapidly develop parasitemia and cerebral symptoms and typically die within 7–12 days. As seen from our initial analysis of the *Pb*A genome (Table S1), much like *P. falciparum*, *Pb*A is very AT rich (76%), with a large number of AT-rich motifs (~5266). In order to define the role of type I IFNs in this model, we infected wild-type mice and *Ifnar1*$^{-/-}$ mice with 1×10^5 parasites of the *PbA*. Parasite loads, survival, and development of neurological symptoms typically associated with cerebral progression were monitored over a 22 day period. No differences in parasitemia were observed in the two strains of mice up to the time of death (data not shown). Of the 27 wild-type animals infected, all were dead by day 12; in all but one of these animals, we observed gross neurological abnormalities. In contrast, of the 22 *Ifnar1*$^{-/-}$ mice tested, all but one survived. (Figure 7E). This difference in outcome was highly statistically significant ($p < 0.0001$). Furthermore, *PbA* infections in *Irf3*$^{-/-}$*Irf7*$^{-/-}$ mice also revealed that these transcription factors are necessary for the progression of cerebral malaria in mouse models, given that mice deficient for these factors survived longer than the wild-type mice (Figure 7F). Similar observations were made when TBK1 hypomorphic mice (*Tbk1*$^{\Delta/\Delta}$), as described previously (Marchlik et al., 2010), were used (Figure 7G). These data indicate that the TBK1-IRF3-IRF7 dependent production of type I IFN and subsequent IFN signaling play an important role in the pathogenesis of cerebral malaria.

DISCUSSION

As all organisms are defined by their nucleic acids, it should not be surprising that nucleic acids have emerged as key triggers of innate immunity. In this report, we have identified a DNA sensing pathway important in innate immunity to malaria. This pathway does not involve any of the known DNA receptors described to date but otherwise follows a core STING-TBK1-IRF signaling pathway. Plasmodial DNA activates this AT-rich stem-loop DNA sensing pathway either as single stranded or double stranded in a sequence-specific manner.

It is probable that AT-rich stem-loop DNA only activates this STING-dependent pathway when it finds its way into the cytosol. Experimentally, this was achieved with a transfection reagent such as lipofectamine. Our previously published findings, that *plasmodial* DNA signals in DCs via TLR9, were explored with DOTAP (Parroche et al., 2007), a transfection reagent that preferentially targets DNA to the endolysosomal compartment. In the absence of transfection reagents, a key question is how DNA could gain access to cytosolic sensors during an actual infection. We propose that hemozoin acts as a vehicle to deliver DNA to a subcellular compartment in which it can have biological effects. This may be particularly relevant because during *Plasmodium* infections, concentrations achieved by free hemozoin in the blood approach 0.2–1mg/ml (Hänscheid et al., 2007). Upon uptake into an immune cell, hemozoin traffics to the phagolysosomal compartment, and TLR9 appears to gain access there to the CpG motifs on the crystalline surface (Parroche et al., 2007). The hemozoin crystal itself activates the cytosolic NLRP3 inflammasome (Dostert et al., 2009; Griffith et al.,

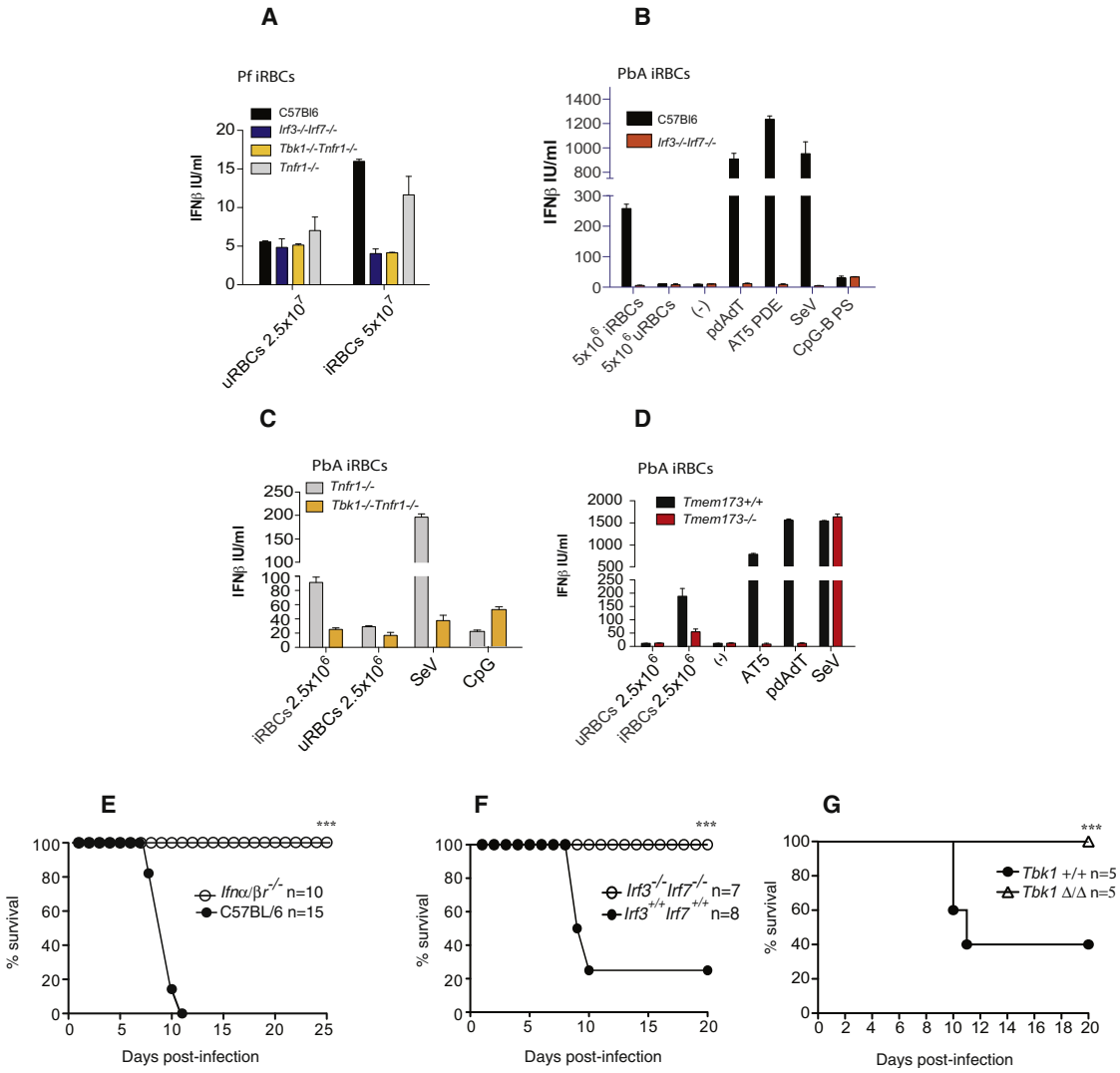

Figure 7. Role of STING, TBK1, and the Transcription Factors IRF3-IRF7 in Plasmodium-Induced IFN Responses In Vitro and In Vivo

(A) *Pf* -infected RBCs (iRBCs) or uninfected RBCs (uRBCs) were incubated with C57Bl/6, *Irf3*$^{-/-}$*Irf7*$^{-/-}$, *Tbk1*$^{-/-}$*Tnfr1*$^{-/-}$, and *Tnfr1*$^{-/-}$ BMDMs as indicated.

(B–D) *Plasmodium berghei* ANKA (PbA) iRBCs were incubated with BMDMs from *Irf3*$^{-/-}$*Irf7*$^{-/-}$, *Tbk1*$^{-/-}$*Tnfr1*$^{-/-}$, *Tnfr1*$^{-/-}$ and *Tmem173*$^{-/-}$ mice for 48 hr and IFN-β induction was measured by ELISA.

(E–G) C57BL/6 (n = 15), *Ifnar*$^{-/-}$ (n = 10), *Irf3*$^{-/-}$*Irf7*$^{-/-}$ (n = 7), *Irf3*$^{+/+}$*Irf7*$^{+/+}$ (n = 8), *Tbk1*$^{+/+}$ (n = 5), and *Tbk1*$^{\Delta/\Delta}$ (n = 5) mice were infected i.p. with 10^5 parasites of *P. berghei ANKA* strain and mice were monitored daily for survival as shown. (***$p \leq 0.0001$, Student's t test). A representative of three independent experiments is shown ± SD.

2009; Shio et al., 2009). One of the mechanisms by which NLRP3 is activated by crystals such as hemozoin, silica, and uric acid is a result of their ability to destabilize the phagolysosome, which allows the delivery of phagosomal contents, including cathepsins, to the cytosol (Halle et al., 2008; Hornung et al., 2008). Phagosomal destabilization probably delivers the AT-rich stem-loop DNA into the cytosol, in which it could then interact with its cytosolic sensor. Indeed, we have observed that hemozoin causes phagolysosomal instability and allows the contents of this compartment, such as the hemozoin crystal and potentially *P. falciparum* DNA on its crystalline surface, access to the cytosol. These observations suggest that after the uptake of DNA-coated hemozoin, sequential activation of a TLR9-dependent response in the phagolysosome and a TLR9-independent response in the cytosol are likely to occur. This observation is supported by the fact that components of both the TLR9 pathway (namely MyD88) as well as those of the STING-dependent DNA response contribute to the IFN response to parasite-laden RBCs. Whereas the defect in Tmem173-deficient cells was incomplete, we found a complete defect in type I IFN induction in *Tbk1*$^{-/-}$ and *Irf3*$^{-/-}$*Irf7*$^{-/-}$ macrophages. Moreover, in line with its previous role in conferring TLR-independent sensitivity to DNA vaccines (Ishii et al., 2008), TBK1 is critical in the development of ECM, probably through the induction of TLR-independent pathways. Thus, our study suggests that two innate pathways are initiated during malaria: a TLR9- and a STING-driven

pathway, both of which converge on the IRFs to regulate IFN gene transcription.

A number of reports have revealed the ability of *Plasmodium spp* to induce type I IFNs and a type I IFN gene signature (Aucan et al., 2003; Pichyangkul et al., 2004; Vigário et al., 2007; Voisine et al., 2010). Previous reports have shown that exogenous recombinant IFN-α can even inhibit ECM and reduce parasite burden in mice infected with *P. berghei* ANKA (*PbA*) (Vigário et al., 2007), although this effect requires pretreatment and is reminiscent of the ability of LPS, for example, to prevent Gram-negative sepsis in mice.

Although, pDCs are typically considered major sources of IFN-α during microbial infections, recent studies indicate that pDCs are not important in regulating immunity to *P. chaubadi* and *PbA* infections (deWalick et al., 2007; Voisine et al., 2010). In the case of *P. chaubadi*, this observation is not surprising because these mice also do not benefit from the loss of the type I IFN receptor (Voisine et al., 2010), but in mice infected with *PbA*, this is a surprise, given the central role pDCs have in generating type I IFNs. Thus, alternative sources of IFN-β, probably mediated by cells other than pDCs via the cytosolic AT-rich ODN pathway, may account for the apparent pathology mediated by the type I IFNs in cerebral malaria, thus explaining the lack of importance of pDCs in ECM models and perhaps in human cerebral malaria.

The importance of DNA recognition and type I interferon production is only now beginning to be appreciated in a large spectrum of infectious illnesses well beyond the traditional role of IFN-α/β in antiviral immunity. The data in this paper are suggestive that plasmodial DNA has the capability of generating type I IFN (as well as proinflammatory cytokines), which in turn determine the outcome of disease. This view of the pathophysiology of malaria is in agreement with the effect of polymorphisms in the human IFN receptors on clinical infections (Aucan et al., 2003; Koch et al., 2002; Naka et al., 2009) as well as by our observation that patients with malaria express a panoply of interferon-stimulated genes. A further observation is that by our analysis, *P. vivax*, although seldom fatal, has a preponderance of both AT motifs ($\sim$5500) as well as CpG motifs ($\sim$3000) (data not shown). In contrast, *Pf*, most often associated with fatal malaria, has a rather large number of AT motifs ($\sim$6000) but much smaller numbers of CpG motifs ($\sim$300) (data not shown). The importance of this distribution is not immediately clear and may further shift our perception of DNA as a pathogen-associated molecular pattern (PAMP) useful in resolving disease.

In view of these results, as well as the emerging literature on DNA sensing, we predict that immune recognition of DNA will be an increasingly common theme in pathogenesis. Microbes as diverse as *Listeria monocytogenes* (O'Connell et al., 2004; Rayamajhi et al., 2010), *Staphylococcus aureus* (Martin et al., 2009), Group B streptococcus (*Streptococcus agalactiae*) (Charrel-Dennis et al., 2008) (Xiao et al., 2009) and *Trypanosoma cruzi* (Chessler et al., 2008) all seem to induce significant amounts of type I IFN through nucleotide recognition. This then suggests that any immunomodulatory therapy contemplated for use as an adjunct for any infectious disease will need to take into account the role of DNA-induced type I IFN in a specific disease and whether or not type I IFNs promote a healthy outcome or enhance pathogenesis.

EXPERIMENTAL PROCEDURES

Mice

Tlr9$^{-/-}$, *Myd88*$^{-/-}$, and *Ticam1*$^{-/-}$ mice (gift of S. Akira, Osaka, Japan) were used for generating *Myd88*$^{-/-}$-*Ticam1*$^{-/-}$ mice. *Dai*$^{-/-}$ and *Irf3*$^{-/-}$-*Irf7*$^{-/-}$ mice were generated from *Irf3*$^{-/-}$ and *Irf7*$^{-/-}$ (gift of T. Taniguchi, Tokyo, Japan). *Tbk1*$^{-/+}$ mice from W.C. Yeh (University of Toronto, Ontario, Canada) were bred with *Tnfr1*$^{-/-}$ mice for generating a double KO. TBK1$^{\Delta/\Delta}$ mice were from Pfizer Pharmaceuticals (MA) (Marchlik et al., 2010). *Ddx58*$^{-/-}$ mice were from S. Akira. *Ifih1*$^{-/-}$ mice were from M. Colonna (Washington University, St. Louis, MI). *Mavs*$^{-/-}$ mice were from of Z.J. Chen (South Western Medical School, Dallas, TX), whereas *Tmem173*$^{-/-}$ mice were from G. Barber. C57BL/6, *Irf1*$^{-/-}$< and *Irf5*$^{-/-}$ mice were from Jackson Laboratories (Bar Harbor, ME). *Ikk*$\varepsilon^{-/-}$-deficient mice were from Millenium Pharmaceuticals (Cambridge, MA). All mouse strains were bred and maintained under specific pathogen-free conditions in the animal facilities at the UMass Medical School in accordance with the Institutional Animal Care and Use Committee.

Reagents

CpG 2007 and 1826 were from Coley Pharmaceuticals, (Wellesley, MA). DOTAP was from Roche (Indianapolis, IN) and Lipofectamine 2000 was from Invitrogen (Carlsbad, CA). Poly(dAdT)•Poly(dAdT) and poly(I:C) were from Sigma-Aldrich and Imigenex, respectively. Lysotracker was from Molecular Probes or Invitrogen (Carlsbad, CA). Forward and reverse strands of interferon stimulating DNA (Stetson and Medzhitov, 2006) were obtained from IDT (Coralville, IA). *Pf* 3D7 gDNA was obtained from the malaria research and reference reagent resource center (MR4) at NIAID. Human embryonic kidney 293 cells were obtained from ATCC (Manassas, VA). ML60218 was from Calbiochem.

Cell Culture, Stimulation, and Microscopy

Mouse bone marrow-derived macrophages, human PBMCs, primary cells, HEK293, and THP-1s were cultured as described (Hornung et al., 2009; Rathinam et al., 2010). Splenocytes and pan-DC subpopulations were isolated from spleens as described (Goutagny et al., 2010). For stimulations, poly(dA-dT) (1 μg/ml), ISD (3 μM), and AT-r stem-loop DNA (3 μM) were transfected with lipofectamine 2000 in accordance with the manufacturer's instructions. Newcastle Disease Virus (NDV, LaSota strain) was obtained from P. Pitha (Johns Hopkins, Baltimore, MD). Sendai Virus (SeV, Cantrell strain) was from Charles River Laboratories (Wilmington, MA). A total of 1×10^5 macrophages were plated with indicated numbers of *Pf*- or PbA-infected RBCs or uninfected RBCs for 48 hr. For immunofluoresence 5×10^5 macrophages in a confocal dish were stimulated with 200 μM natural hemozoin for 1 and 6 hr. Lysotracker (Molecular Probes or Invitrogen) was added to cells at a final dilution of 1:10000 in media for 15 min for visualization of the lysosomes. Specifically hemozoin in cells was visualized with acousto-reflection microscopy with a Leica SP2 microscope as described (Hornung et al., 2008).

RNA Extraction and Real-Time PCR

Human PBMC, mouse BMDM, HEK293, or mouse splenocytes (3 to 10×10^6 cells/condition), were stimulated for 6 to 17 hr with hemozoin (100 μM) or poly(dA-dT) (5 μg/ml), CpG motifs (5 μM), AT-rich ODNs (3 μM), or *Pf* gDNA (5 μg), all of which were transfected with lipofectamine 2000 (Invitrogen). RNA was extracted with RNeasy kit (QIAGEN, CA), cDNA was synthesized, and quantitative RT-PCR analysis was performed with primers as described (Charrel-Dennis et al., 2008; Goutagny et al., 2010). Gene expression data are presented as a ratio of gene copy number per 100 copies of Actin ± SD.

P. falciparum Culture

Erythrocytic stages of *Pf* 3D7 isolates were cultured and natural hemozoin and DNA from *Pf* were purified as described (Parroche et al., 2007). For iRBC preparation, malaria cultures were synchronized with sorbitol for 3 cycles. *Pf* culture stage and parasitemia was assessed daily by field staining. Where indicated, *Pf* enriched cultures at 8% parasitemia and trophozoite or schizont stages were purified as described (Baratin et al., 2005; Cooper et al., 2005; Wu et al., 2010). The culture was then adjusted to a parasitemia of 8% and used for stimulating PBMCs at 40% hematocrit.

P. berghei ANKA Induced Cerebral Malaria Model

The *P. berghei ANKA* (Pba) strain (gift of A. Luster, Harvard, Boston, MA) was maintained by passage in C57BL/6 mice. Mice were inoculated i.p. with 1×10^5 infected RBCs and neurological symptoms and death were recorded daily. Cerebral malaria was diagnosed by clinical signs including ataxia, paralysis, deviation of the head, convulsions, and coma, followed by death. Moribund animals were scored as dead and euthanized. For ex vivo infections with PbA iRBCs, BALB/c mice were injected with PbA at 1×10^5 iRBCs and parasitemia was monitored daily. Blood was collected by cardiac puncture at 65% parasitemia.

Design of *P. falciparum* AT Motifs and Secondary Structure Modeling

Twenty-mer AT ODNs containing the consensus motif 5′-NNNNNNATTTTT ACNNNNNN-3′ were identified in the *Pf* genome using Fuzznuc, an algorithm from the EMBOSS package (http://emboss.sourceforge.net/apps/release/6.2/emboss/apps/fuzznuc.html). The Fuzznuc reverse option was enabled so that both DNA strands were screened. All AT-rich ODNs, including biotin-labeled ODNs, were synthesized by IDT (San Jose, CA) and tested on both phosphodiester (PD) and phosphorothiorate (PS) backbones in different cell types. All AT-rich stem-loop DNA sequences were uploaded on mFold (M. Zuker) and secondary structure modeling was carried out at 37°C and default [Mg^{2+}].

Microarray Analysis

Human studies were approved by the University of Massachusetts Medical School Institutional Review Board, the local IRBs of the Brazilian institutions and the Brazilian national IRB (CONEP approval number 10567). Portions of the microarray analysis have been previously reported (Franklin et al., 2009) where the methodology is reported in detail. The current study represents 14 otherwise healthy patients (from Porto Vehlo, Brazil) who were naturally infected with *P. falciparum* before and 3–5 weeks after documented curative treatment with mefloquine. Each patient served as his/her own control. PCR was used for excluding patients with mixed infections involving *P. vivax*. Simple filtering, normalization and averaging were carried out with BASE (Bio-Array Software Environment) (https://base.mgh.har vard.edu/) and log transformed (log2). Genes were filtered to include only genes with a signal greater than the average signal from the negative controls in at least one of the samples with a detection p value less than 0.0,1. Differences in gene expression between the two conditions were considered significant if $p < 0.01$ with a paired t test with Benjamini-Hochberg correction for multiple testing and a fold change greater than 1.7.

ELISA

Cell culture supernatants were assayed for huIFN-α by ELISA (R&D or Bender MedSystems), in accordance with the manufacturer's instructions. The mouse TNF-α and IL-6 kits were from eBiosciences, whereas the murine IFN-β kit is as described (Roberts et al., 2007).

Reporter Assays

HEK293 cells (2×10^4 cells/well), were plated in 96 well plates and stimulated for 24 hr as outlined above, and IFN-β, PRDIII-I, PPRD-II, PRD-IV, and NF-kB luciferase reporter activity were measured as described (Rothenfusser et al., 2005). The full-length IFN-β promoter and PRDIII-I, PRDII, and PRDIV luciferase reporters were from T. Maniatis (Harvard University, Boston, MA). pGL4-TK Renilla luciferase and pGL3-control luciferase were from Promega (Madison, WI). pME18-NS3/4A-myc and NS3/4S139A-myc were from Z.J. Chen (UT Southwestern, Dallas, Texas). The pGL3-enhancer-ELAM-minimal promoter was used for assessing NF-κB activity.

RNA Preparation and Nanostring Experiment

If not indicated otherwise, DNA-transfected or SeV-infected 293 cells (2.4×10^5 cells per 12 wells) were collected 9 hr or 18 hr after stimulation. The Mini RNA Isolation II Kit (Zymo Research) was used for RNA isolation with the previously described modifications (Ablasser et al., 2009). nCounter CodeSets were constructed for detecting selected mouse-specific genes as described previously (Dixit et al., 2010). A total of 2×10^5 BMDMs from *Tmem173*$^{+/+}$ and *Tmem173*$^{-/-}$ animals were lysed in RLT buffer (QIAGEN) supplemented with β-mercaptoethanol. Five percent of this lysate (containing 10^4 cells) was hybridized to the Codeset for 16 hr and loaded onto the nCounter prep station, and then quantified with the nCounter Digital Analyzer. For side-by-side comparisons of nCounter experiments, data was normalized in two ways described previously (Dixit et al., 2010).

RNA-Mediated Interference

First, siRNA was reverse-transfected at a concentration of 25 nM into TLR3$^+$-HEK293 cells (4×10^4 cells per 96 wells) with 0.5 μl lipofectamine. Forty-eight hours after transfection, cells were stimulated and after an additional period of 24 hr levels of IFN-β mRNA were assessed with RT-PCR. Poly(I:C) was added at 100 ng/ml final concentration, while transfected poly(I:C) was introduced at 10ng/ml. siRNA sequences used for RNA-polymerase III, MAVS, RIG-I, and STING were obtained from QIAGEN or Invitrogen and are as described (Ablasser et al., 2009; Ishikawa and Barber, 2008).

Pull-down Assays and Immunoblotting

A total of 3×10^6 HEK293 cells or *Tmem173*$^{-/-}$, *Tmem173*$^{+/+}$, *Tbk1*$^{-/-}$ *Tnfr1*$^{-/-}$, and *Tnfr1*$^{-/-}$ BMDMs were lysed with lysis buffer containing NP-40, dithiothreitol (DTT), phenylmethylsulfonyl fluoride (PMSF), and sodium orthovanadate (Na_3VO_4) for 20 min at 4°C. Lysates were spun for debris removal and then incubated with 1 μg of 3′ or 5′-biotinylated AT2 (PS) or AT5 (PD) and streptavidin-agarose beads (50% w/v) for 2 hr. Lysates were spun for obtaining the bead pellet, washed, and boiled with loading buffer containing SDS and run on 10% SDS-polyacrylamide gel. Blots were probed with the STING antibody as described (Ishikawa and Barber, 2008); anti-TBK1 was obtained from Imgenex and anti-β-actin was from Sigma.

ShRNA-Mediated Silencing

The lentiviral shRNA sequences were cloned into pLKO.1 TRC cloning vector 56. The silencing sequence was from the MISSION TRC-Hs 1.0 (Human) as follows: TRCN0000-123051 for DAI. The production of viral particles and transduction of target cells were conducted according to the following protocols (http://www.broad.mit.edu/genome_bio/trc/publicProtocols.html). Knockdown efficiency was assessed by one-step RT-PCR (Invitrogen) with the following primers: DAI-F 5′-ATCTGCCTGGAGTTACCTTC-3′; DAI-R 5′-TCTGGATTTCCTGACCTATTG-3′ and antibody to DAI (Imgenex).

Statistical Analysis

Differences between groups were analyzed for statistical significance with Student's t test. $p < 0.05$ was considered as statistically significant.

ACCESSION NUMBERS

The microarray data are available in the Gene Expression Omnibus (GEO) database (http://www.ncbi.nlm.nih.gov/gds) under the accession number GSE15221.

SUPPLEMENTAL INFORMATION

Supplemental Information includes six figures and two tables and can be found with this article online at doi:10.1016/j.immuni.2011.05.016.

ACKNOWLEDGMENTS

The authors would like to thank A. Cerny for animal husbandry and genotyping and O. Mulhern for her help with affinity purification assays. This work is supported by NIH grants AI067497 (to K.A.F), by AI079293 (to K.A.F and D.T.G), by R21AI80907 (to R.T.G) and FAPEMIG/CNPq/INCTV from FIOCRUZ, Brazil (to D.T.G). K.A.F and D.T.G oversaw the whole project with R.T.G and S.S. S.S. designed and conducted the experiments with help from Z.J., R.O., P.P., P.K., F.L., and N.G. D.C.B quantified the AT-rich and CpG motif frequency, R.O. and J.C. conducted the in vivo mouse models, and H.B. performed microarray analysis. G.B. made STING-deficient mice and J.P.H made the TBK1-hypomorphic mice. S.S., K.A.F., and D.T.G. wrote the manuscript.

Received: April 21, 2010
Revised: April 28, 2011
Accepted: May 16, 2011
Published online: August 4, 2011

REFERENCES

Ablasser, A., Bauernfeind, F., Hartmann, G., Latz, E., Fitzgerald, K., and Hornung, V. (2009). RIG-I-dependent sensing of poly(dA:dT) through the induction of an RNA polymerase III-transcribed RNA intermediate. Nat. Immunol. *10*, 1065–1072.

Adachi, K., Tsutsui, H., Kashiwamura, S., Seki, E., Nakano, H., Takeuchi, O., Takeda, K., Okumura, K., Van Kaer, L., Okamura, H., et al. (2001). Plasmodium berghei infection in mice induces liver injury by an IL-12- and toll-like receptor/myeloid differentiation factor 88-dependent mechanism. J. Immunol. *167*, 5928–5934.

Aucan, C., Walley, A.J., Hennig, B.J., Fitness, J., Frodsham, A., Zhang, L., Kwiatkowski, D., and Hill, A.V. (2003). Interferon-alpha receptor-1 (IFNAR1) variants are associated with protection against cerebral malaria in the Gambia. Genes Immun. *4*, 275–282.

Baratin, M., Roetynck, S., Lépolard, C., Falk, C., Sawadogo, S., Uematsu, S., Akira, S., Ryffel, B., Tiraby, J.G., Alexopoulou, L., et al. (2005). Natural killer cell and macrophage cooperation in MyD88-dependent innate responses to Plasmodium falciparum. Proc. Natl. Acad. Sci. USA *102*, 14747–14752.

Bonnard, M., Mirtsos, C., Suzuki, S., Graham, K., Huang, J., Ng, M., Itié, A., Wakeham, A., Shahinian, A., Henzel, W.J., et al. (2000). Deficiency of T2K leads to apoptotic liver degeneration and impaired NF-kappaB-dependent gene transcription. EMBO J. *19*, 4976–4985.

Charrel-Dennis, M., Latz, E., Halmen, K.A., Trieu-Cuot, P., Fitzgerald, K.A., Kasper, D.L., and Golenbock, D.T. (2008). TLR-independent type I interferon induction in response to an extracellular bacterial pathogen via intracellular recognition of its DNA. Cell Host Microbe *4*, 543–554.

Chessler, A.D., Ferreira, L.R., Chang, T.H., Fitzgerald, K.A., and Burleigh, B.A. (2008). A novel IFN regulatory factor 3-dependent pathway activated by trypanosomes triggers IFN-beta in macrophages and fibroblasts. J. Immunol. *181*, 7917–7924.

Chiu, Y.H., Macmillan, J.B., and Chen, Z.J. (2009). RNA polymerase III detects cytosolic DNA and induces type I interferons through the RIG-I pathway. Cell *138*, 576–591.

Clark, I.A., Alleva, L.M., Mills, A.C., and Cowden, W.B. (2004). Pathogenesis of malaria and clinically similar conditions. Clin. Microbiol. Rev. *17*, 509–539.

Cooper, R.A., Papakrivos, J., Lane, K.D., Fujioka, H., Lingelbach, K., and Wellems, T.E. (2005). PfCG2, a Plasmodium falciparum protein peripherally associated with the parasitophorous vacuolar membrane, is expressed in the period of maximum hemoglobin uptake and digestion by trophozoites. Mol. Biochem. Parasitol. *144*, 167–176.

Der, S.D., Zhou, A., Williams, B.R., and Silverman, R.H. (1998). Identification of genes differentially regulated by interferon alpha, beta, or gamma using oligonucleotide arrays. Proc. Natl. Acad. Sci. USA *95*, 15623–15628.

deWalick, S., Amante, F.H., McSweeney, K.A., Randall, L.M., Stanley, A.C., Haque, A., Kuns, R.D., MacDonald, K.P., Hill, G.R., and Engwerda, C.R. (2007). Cutting edge: Conventional dendritic cells are the critical APC required for the induction of experimental cerebral malaria. J. Immunol. *178*, 6033–6037.

Dixit, E., Boulant, S., Zhang, Y., Lee, A.S., Odendall, C., Shum, B., Hacohen, N., Chen, Z.J., Whelan, S.P., Fransen, M., et al. (2010). Peroxisomes are signaling platforms for antiviral innate immunity. Cell *141*, 668–681.

Dostert, C., Guarda, G., Romero, J.F., Menu, P., Gross, O., Tardivel, A., Suva, M.L., Stehle, J.C., Kopf, M., Stamenkovic, I., et al. (2009). Malarial hemozoin is a Nalp3 inflammasome activating danger signal. PLoS ONE *4*, e6510.

Fitzgerald, K.A., McWhirter, S.M., Faia, K.L., Rowe, D.C., Latz, E., Golenbock, D.T., Coyle, A.J., Liao, S.M., and Maniatis, T. (2003). IKKepsilon and TBK1 are essential components of the IRF3 signaling pathway. Nat. Immunol. *4*, 491–496.

Foy, E., Li, K., Sumpter, R., Jr., Loo, Y.M., Johnson, C.L., Wang, C., Fish, P.M., Yoneyama, M., Fujita, T., Lemon, S.M., and Gale, M., Jr. (2005). Control of antiviral defenses through hepatitis C virus disruption of retinoic acid-inducible gene-I signaling. Proc. Natl. Acad. Sci. USA *102*, 2986–2991.

Franklin, B.S., Rodrigues, S.O., Antonelli, L.R., Oliveira, R.V., Goncalves, A.M., Sales-Junior, P.A., Valente, E.P., Alvarez-Leite, J.I., Ropert, C., Golenbock, D.T., and Gazzinelli, R.T. (2007). MyD88-dependent activation of dendritic cells and CD4(+) T lymphocytes mediates symptoms, but is not required for the immunological control of parasites during rodent malaria. Microbes Infect. *9*, 881–890.

Franklin, B.S., Parroche, P., Ataíde, M.A., Lauw, F., Ropert, C., de Oliveira, R.B., Pereira, D., Tada, M.S., Nogueira, P., da Silva, L.H., et al. (2009). Malaria primes the innate immune response due to interferon-gamma induced enhancement of toll-like receptor expression and function. Proc. Natl. Acad. Sci. USA *106*, 5789–5794.

Gardner, M.J., Hall, N., Fung, E., White, O., Berriman, M., Hyman, R.W., Carlton, J.M., Pain, A., Nelson, K.E., Bowman, S., et al. (2002). Genome sequence of the human malaria parasite Plasmodium falciparum. Nature *419*, 498–511.

Gazzinelli, R.T., Ropert, C., and Campos, M.A. (2004). Role of the Toll/interleukin-1 receptor signaling pathway in host resistance and pathogenesis during infection with protozoan parasites. Immunol. Rev. *201*, 9–25.

Goutagny, N., Jiang, Z., Tian, J., Parroche, P., Schickli, J., Monks, B.G., Ulbrandt, N., Ji, H., Kiener, P.A., Coyle, A.J., and Fitzgerald, K.A. (2010). Cell type-specific recognition of human metapneumoviruses (HMPVs) by retinoic acid-inducible gene I (RIG-I) and TLR7 and viral interference of RIG-I ligand recognition by HMPV-B1 phosphoprotein. J. Immunol. *184*, 1168–1179.

Griffith, J.W., Sun, T., McIntosh, M.T., and Bucala, R. (2009). Pure Hemozoin is inflammatory in vivo and activates the NALP3 inflammasome via release of uric acid. J. Immunol. *183*, 5208–5220.

Halle, A., Hornung, V., Petzold, G.C., Stewart, C.R., Monks, B.G., Reinheckel, T., Fitzgerald, K.A., Latz, E., Moore, K.J., and Golenbock, D.T. (2008). The NALP3 inflammasome is involved in the innate immune response to amyloid-beta. Nat. Immunol. *9*, 857–865.

Hänscheid, T., Egan, T.J., and Grobusch, M.P. (2007). Haemozoin: From melatonin pigment to drug target, diagnostic tool, and immune modulator. Lancet Infect. Dis. *7*, 675–685.

Honda, K., and Taniguchi, T. (2006). IRFs: Master regulators of signalling by Toll-like receptors and cytosolic pattern-recognition receptors. Nat. Rev. Immunol. *6*, 644–658.

Hornung, V., Bauernfeind, F., Halle, A., Samstad, E.O., Kono, H., Rock, K.L., Fitzgerald, K.A., and Latz, E. (2008). Silica crystals and aluminum salts activate the NALP3 inflammasome through phagosomal destabilization. Nat. Immunol. *9*, 847–856.

Hornung, V., Ablasser, A., Charrel-Dennis, M., Bauernfeind, F., Horvath, G., Caffrey, D.R., Latz, E., and Fitzgerald, K.A. (2009). AIM2 recognizes cytosolic dsDNA and forms a caspase-1-activating inflammasome with ASC. Nature *458*, 514–518.

Ishii, K.J., Kawagoe, T., Koyama, S., Matsui, K., Kumar, H., Kawai, T., Uematsu, S., Takeuchi, O., Takeshita, F., Coban, C., and Akira, S. (2008). TANK-binding kinase-1 delineates innate and adaptive immune responses to DNA vaccines. Nature *451*, 725–729.

Ishikawa, H., and Barber, G.N. (2008). STING is an endoplasmic reticulum adaptor that facilitates innate immune signalling. Nature *455*, 674–678.

Ishikawa, H., Ma, Z., and Barber, G.N. (2009). STING regulates intracellular DNA-mediated, type I interferon-dependent innate immunity. Nature *461*, 788–792.

Kawai, T., Takahashi, K., Sato, S., Coban, C., Kumar, H., Kato, H., Ishii, K.J., Takeuchi, O., and Akira, S. (2005). IPS-1, an adaptor triggering RIG-I- and Mda5-mediated type I interferon induction. Nat. Immunol. *6*, 981–988.

Khor, C.C., Chapman, S.J., Vannberg, F.O., Dunne, A., Murphy, C., Ling, E.Y., Frodsham, A.J., Walley, A.J., Kyrieleis, O., Khan, A., et al. (2007). A Mal functional variant is associated with protection against invasive pneumococcal disease, bacteremia, malaria and tuberculosis. Nat. Genet. *39*, 523–528.

Koch, O., Awomoyi, A., Usen, S., Jallow, M., Richardson, A., Hull, J., Pinder, M., Newport, M., and Kwiatkowski, D. (2002). IFNGR1 gene promoter polymorphisms and susceptibility to cerebral malaria. J. Infect. Dis. *185*, 1684–1687.

Marchlik, E., Thakker, P., Carlson, T., Jiang, Z., Ryan, M., Marusic, S., Goutagny, N., Kuang, W., Askew, G.R., Roberts, V., et al. (2010). Mice lacking Tbk1 activity exhibit immune cell infiltrates in multiple tissues and increased susceptibility to LPS-induced lethality. J. Leukoc. Biol. *88*, 1171–1180.

Martin, F.J., Gomez, M.I., Wetzel, D.M., Memmi, G., O'Seaghdha, M., Soong, G., Schindler, C., and Prince, A. (2009). Staphylococcus aureus activates type I IFN signaling in mice and humans through the Xr repeated sequences of protein A. J. Clin. Invest. *119*, 1931–1939.

Meylan, E., Curran, J., Hofmann, K., Moradpour, D., Binder, M., Bartenschlager, R., and Tschopp, J. (2005). Cardif is an adaptor protein in the RIG-I antiviral pathway and is targeted by hepatitis C virus. Nature *437*, 1167–1172.

Mockenhaupt, F.P., Cramer, J.P., Hamann, L., Stegemann, M.S., Eckert, J., Oh, N.R., Otchwemah, R.N., Dietz, E., Ehrhardt, S., Schröder, N.W., et al. (2006). Toll-like receptor (TLR) polymorphisms in African children: Common TLR-4 variants predispose to severe malaria. Proc. Natl. Acad. Sci. USA *103*, 177–182.

Naka, I., Patarapotikul, J., Hananantachai, H., Tokunaga, K., Tsuchiya, N., and Ohashi, J. (2009). IFNGR1 polymorphisms in Thai malaria patients. Infect. Genet. Evol. *9*, 1406–1409.

Neill, A.L., and Hunt, N.H. (1992). Pathology of fatal and resolving Plasmodium berghei cerebral malaria in mice. Parasitology *105*, 165–175.

O'Connell, R.M., Saha, S.K., Vaidya, S.A., Bruhn, K.W., Miranda, G.A., Zarnegar, B., Perry, A.K., Nguyen, B.O., Lane, T.F., Taniguchi, T., et al. (2004). Type I interferon production enhances susceptibility to Listeria monocytogenes infection. J. Exp. Med. *200*, 437–445.

Panne, D., Maniatis, T., and Harrison, S.C. (2007). An atomic model of the interferon-beta enhanceosome. Cell *129*, 1111–1123.

Parroche, P., Lauw, F.N., Goutagny, N., Latz, E., Monks, B.G., Visintin, A., Halmen, K.A., Lamphier, M., Olivier, M., Bartholomeu, D.C., et al. (2007). Malaria hemozoin is immunologically inert but radically enhances innate responses by presenting malaria DNA to Toll-like receptor 9. Proc. Natl. Acad. Sci. USA *104*, 1919–1924.

Pichyangkul, S., Yongvanitchit, K., Kum-arb, U., Hemmi, H., Akira, S., Krieg, A.M., Heppner, D.G., Stewart, V.A., Hasegawa, H., Looareesuwan, S., et al. (2004). Malaria blood stage parasites activate human plasmacytoid dendritic cells and murine dendritic cells through a Toll-like receptor 9-dependent pathway. J. Immunol. *172*, 4926–4933.

Rathinam, V.A., Jiang, Z., Waggoner, S.N., Sharma, S., Cole, L.E., Waggoner, L., Vanaja, S.K., Monks, B.G., Ganesan, S., Latz, E., et al. (2010). The AIM2 inflammasome is essential for host defense against cytosolic bacteria and DNA viruses. Nat. Immunol. *11*, 395–402.

Rayamajhi, M., Humann, J., Penheiter, K., Andreasen, K., and Lenz, L.L. (2010). Induction of IFN-alphabeta enables Listeria monocytogenes to suppress macrophage activation by IFN-gamma. J. Exp. Med. *207*, 327–337.

Roberts, Z.J., Goutagny, N., Perera, P.Y., Kato, H., Kumar, H., Kawai, T., Akira, S., Savan, R., van Echo, D., Fitzgerald, K.A., et al. (2007). The chemotherapeutic agent DMXAA potently and specifically activates the TBK1-IRF-3 signaling axis. J. Exp. Med. *204*, 1559–1569.

Rothenfusser, S., Goutagny, N., DiPerna, G., Gong, M., Monks, B.G., Schoenemeyer, A., Yamamoto, M., Akira, S., and Fitzgerald, K.A. (2005). The RNA helicase Lgp2 inhibits TLR-independent sensing of viral replication by retinoic acid-inducible gene-I. J. Immunol. *175*, 5260–5268.

Sabbah, A., Chang, T.H., Harnack, R., Frohlich, V., Tominaga, K., Dube, P.H., Xiang, Y., and Bose, S. (2009). Activation of innate immune antiviral responses by Nod2. Nat. Immunol. *10*, 1073–1080.

Saitoh, T., Fujita, N., Hayashi, T., Takahara, K., Satoh, T., Lee, H., Matsunaga, K., Kageyama, S., Omori, H., Noda, T., et al. (2009). Atg9a controls dsDNA-driven dynamic translocation of STING and the innate immune response. Proc. Natl. Acad. Sci. USA *106*, 20842–20846.

Sanda, C., Weitzel, P., Tsukahara, T., Schaley, J., Edenberg, H.J., Stephens, M.A., McClintick, J.N., Blatt, L.M., Li, L., Brodsky, L., and Taylor, M.W. (2006). Differential gene induction by type I and type II interferons and their combination. J. Interferon Cytokine Res. *26*, 462–472.

Shimosato, T., Kimura, T., Tohno, M., Iliev, I.D., Katoh, S., Ito, Y., Kawai, Y., Sasaki, T., Saito, T., and Kitazawa, H. (2006). Strong immunostimulatory activity of AT-oligodeoxynucleotide requires a six-base loop with a self-stabilized 5′-C…G-3′ stem structure. Cell. Microbiol. *8*, 485–495.

Shio, M.T., Eisenbarth, S.C., Savaria, M., Vinet, A.F., Bellemare, M.J., Harder, K.W., Sutterwala, F.S., Bohle, D.S., Descoteaux, A., Flavell, R.A., and Olivier, M. (2009). Malarial hemozoin activates the NLRP3 inflammasome through Lyn and Syk kinases. PLoS Pathog. *5*, e1000559.

Stetson, D.B., and Medzhitov, R. (2006). Recognition of cytosolic DNA activates an IRF3-dependent innate immune response. Immunity *24*, 93–103.

Takaoka, A., Wang, Z., Choi, M.K., Yanai, H., Negishi, H., Ban, T., Lu, Y., Miyagishi, M., Kodama, T., Honda, K., et al. (2007). DAI (DLM-1/ZBP1) is a cytosolic DNA sensor and an activator of innate immune response. Nature *448*, 501–505.

Togbe, D., Schofield, L., Grau, G.E., Schnyder, B., Boissay, V., Charron, S., Rose, S., Beutler, B., Quesniaux, V.F., and Ryffel, B. (2007). Murine cerebral malaria development is independent of toll-like receptor signaling. Am. J. Pathol. *170*, 1640–1648.

Unterholzner, L., Keating, S.E., Baran, M., Horan, K.A., Jensen, S.B., Sharma, S., Sirois, C., Jin, T., Xiao, T., Fitzgerald, K.A., et al. (2010). IFI16 is a novel innate immune sensor for cytoplasmic DNA. Nat. Immunol. *11*, 997–1004.

Vigário, A.M., Belnoue, E., Grüner, A.C., Mauduit, M., Kayibanda, M., Deschemin, J.C., Marussig, M., Snounou, G., Mazier, D., Gresser, I., and Rénia, L. (2007). Recombinant human IFN-alpha inhibits cerebral malaria and reduces parasite burden in mice. J. Immunol. *178*, 6416–6425.

Voisine, C., Mastelic, B., Sponaas, A.M., and Langhorne, J. (2010). Classical CD11c+ dendritic cells, not plasmacytoid dendritic cells, induce T cell responses to Plasmodium chabaudi malaria. Int. J. Parasitol. *40*, 711–719.

Wu, X., Gowda, N.M., Kumar, S., and Gowda, D.C. (2010). Protein-DNA Complex Is the Exclusive Malaria Parasite Component that Activates Dendritic Cells and Triggers Innate Immune Responses. J. Immunol. *184*, 4338–4348.

Xiao, N., Eidenschenk, C., Krebs, P., Brandl, K., Blasius, A.L., Xia, Y., Khovananth, K., Smart, N.G., and Beutler, B. (2009). The Tpl2 mutation Sluggish impairs type I IFN production and increases susceptibility to group B streptococcal disease. J. Immunol. *183*, 7975–7983.

Yoneyama, M., and Fujita, T. (2009). RNA recognition and signal transduction by RIG-I-like receptors. Immunol. Rev. *227*, 54–65.

Zhong, B., Yang, Y., Li, S., Wang, Y.Y., Li, Y., Diao, F., Lei, C., He, X., Zhang, L., Tien, P., and Shu, H.B. (2008). The adaptor protein MITA links virus-sensing receptors to IRF3 transcription factor activation. Immunity *29*, 538–550.

Zhu, J., Krishnegowda, G., and Gowda, D.C. (2005). Induction of proinflammatory responses in macrophages by the glycosylphosphatidylinositols of Plasmodium falciparum: The requirement of extracellular signal-regulated kinase, p38, c-Jun N-terminal kinase and NF-kappaB pathways for the expression of proinflammatory cytokines and nitric oxide. J. Biol. Chem. *280*, 8617–8627.